EFFECT OF DIFFERENT CEMENTS AND MIX PROPORTIONS ON RESULTS OBTAINED WITH ACCELERATED ELECTROCHEMICAL LEACHING TEST

(Translation from Proceedings of JSCE, No.564/V-35, May. 1997)


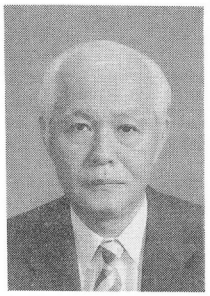
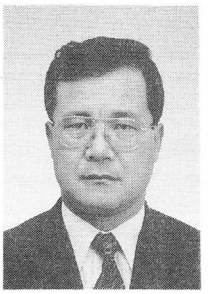


Hiroshi SAITO Sunao NAKANE Yukikazu TSUJI Ai FUJIWARA

Certain facilities such as nuclear waste repositories require that concrete maintains long-term durability while in contact with water. For such structures, it is important to develop a technology for predicting concrete degradation.
An acceleration test method based on an electrochemical technique has been developed. A potential gradient is applied across a specimen to accelerate the dissolution of cement hydrates from the concrete where it is in contact with water. Experimental studies were carried out to clarify the effect of differences in cement type and mix proportions, and these effects are reflected in the results obtained with the test. Three tests parameters were used: sand content, water/cement ratio, and cement type. The test results were considered from the viewpoint of the quantity and quality of cement hydrate. They reflected the differences in materials and mix proportions of the test specimen.

Keywords: *degradation, cement hydrate structure, electrochemical technique, dissolution, mix proportion, cement type*

Hiroshi Saito is a Deputy General Manager in Consulting Department of Technical Research Institute at Obayashi Corporation, Tokyo, Japan. He obtained his D. Eng. from Gunma University in 1998. His research interest relates to durability of concrete from chemical aspect. He is a member of JSCE.

Sunao Nakane is a General Manager in Consulting Department of Technical Research Institute at Obayashi Corporation, Tokyo, Japan. His research interest relates to concrete engineering. He is a member of JSCE.

Yukikazu Tsuji is a Professor in the Department of Civil Engineering at Gunma University. He obtained his D. Eng. from the University of Tokyo in 1974. His research interests include behavior of reinforced concrete structures, chemically pre-stressed concrete, and properties of fresh concrete. He is a member of JSCE.

Ai Fujiwara is a Manager at Radioactive Waste Management Center, Tokyo, Japan. His research interest relates to an engineering barrier system of radioactive waste.

1. INTRODUCTION

Nuclear waste repositories are constructed deep below the surface, and their main degradation factors are a gradual dissolution of cement hydrates in water and chemical attack by components in the ground water that are harmful to concrete. The latter is generally more rapid than the former. However, it is possible to choose repository sites where there is a low concentration of such harmful components. Thus, it is important to investigate the degradation of such structures due to dissolution of cement hydrates.

The authors have carried out experimental studies to develop an electrochemical acceleration test method that clarifies the mechanism of degradation by leaching and a model for simulating the long-term degradation behavior of concrete. With this method, the rate of Ca^{2+} ion migration toward a cathode is accelerated by applying a constant DC potential gradient across a mortar specimen in contact with water. The amount of Ca^{2+} dissolved in water on the cathode side, the degraded thickness, the constituents of the cement hydrates, and the changes in pore structure have been measured. Results demonstrate that this method of accelerated cement hydrate dissolution in water is workable, and that the amount of dissolved Ca^{2+} is proportional to the potential gradient within the range 2 to 10V/cm [1]. This accelerated process reproduced the naturally occurring degradation of cement hydrates, which progresses gradually from the surface to the interior [2]. The relationship between degradation thickness and the amount of dissolved Ca^{2+} is expressed by a linear equation [3].

Other researchers [4,5] have also helped to clarify the feasibility of using an electric field to degrade cement-based materials in contact with water. However, three major tasks must still be completed before the usefulness of this method is fully verified: (1) to determine the effect of cement type and mix proportion on the test results, (2) to determine the possibility of applying the method to the deterioration of concrete by chemical attack using dilute corrosive solutions, and (3) to determine the acceleration rate compared to natural degradation. Materials and mix proportions are the most important factors in concrete durability. Thus, it is necessary to choose them properly in designing a repository. If we want to utilize results obtained by this method for that purpose, they must accurately reflect differences in materials and mix proportions.

It is thought that the amount of dissolved Ca^{2+} and the degraded thickness may be affected by the quantity and quality of the cement hydrates. The amount of hydrates is fixed by the mix proportion, while its quality is determined by the mix proportion and the materials (mainly the cement type). Thus, the applicability of the method would be verified if test results clearly reflected differences in mix proportion and materials, and analysis could then be done from the viewpoint of quality and quantity of the cement hydrates.

Concrete is often used as a barrier and/or structural material, so it is necessary to clarify changes in performance with degradation. It is important to clarify the relationship between changes in performance and changes in cement hydrate structure, because the two are thought to closely correspond.

This report describes accelerated test results for different mortars,

taking into account the quantity of cement hydrates and their structural quality. Also covered are changes in the hydrate structure, permeability, and strength, which are some of the barrier parameters affected by degradation.

2. CEMENT HYDRATE DISSOLUTION MECHANISM AND THE PRINCIPLE OF ELECTROCHEMICAL ACCELERATION

There is a chemical equilibrium between the main cement hydrates $Ca(OH)_2$ and C-S-H, and their component ions in pore water, as described by the following chemical reactions:

$$Ca(OH)_2 = Ca^{2+} + 2OH^- \quad (1)$$

$$C\text{-}S\text{-}H = Ca^{2+} + 2OH^- + SiO_2 \quad (2)$$

Dissolution of cement hydrates causes a shift in the chemical equilibrium toward the right-hand side of these reactions. If the Ca^{2+} or OH^- concentration in the pore water decreases, the chemical equilibrium moves to the right and dissolution of cement hydrate occurs. Brown [6] demonstrated the chemical equilibrium between $Ca(OH)_2$, C-S-H, and their component ions in pore water from the viewpoint of thermodynamics; there is a chemical equilibrium in the pore solution. If the Ca^{2+} concentration in the pore water decreases, $Ca(OH)_2$ dissolves, thus supplying additional Ca^{2+} ions to maintain the equilibrium. After complete dissolution of the $Ca(OH)_2$, Ca^{2+} ions supplemented by the C-S-H start to dissolve and the C-S-H finally degrades to SiO_2 gel. Thus, the two dissolution reactions do not occur simultaneously: $Ca(OH)_2$ dissolves first, then C-S-H.

Furthermore, cement hydrate dissolution seems to correspond to a movement of related ions. This suggests that if dissolution speed is determined by ion movement speed, then dissolution speed could be accelerated by increasing the speed of ion movement. This led to the application of a potential gradient to increase the rate of ion movement. According to electrochemical principles, ions in solution move toward opposite electrodes under a direct-current potential gradient, i.e., cations move toward the cathode and anions move toward the anode. In an infinite dilute solution, the rate of movement under a 1V/cm gradient is defined as the mobility, and each ion has its own characteristic value.

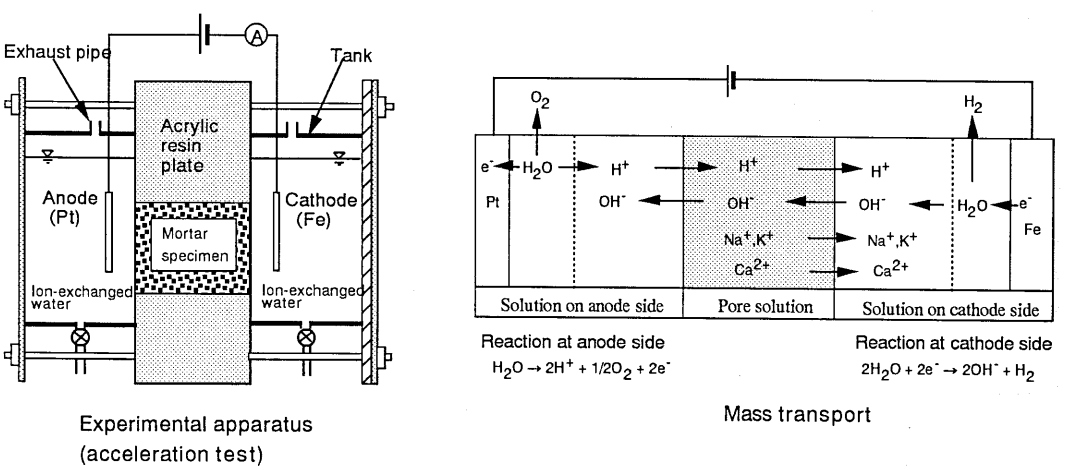

Experimental apparatus (acceleration test)

Mass transport

Fig.1 Experimental apparatus and mass transport in the tests

Fig. 1 shows the experimental apparatus used in the test and the mass transport concept applied. The specimen was clamped between two glass vessels, each containing one liter of ion-exchanged water. Each vessel also had a small pipe for exhausting the gas produced by electrolysis. One vessel contained an anode (Pt) and the other a cathode (stainless steel); these were connected to a DC power source to provide a potential gradient across the specimen. Ca^{2+} ions in the pore solution moved rapidly to the cathode, and thus hastened cement hydrate dissolution. In this electrochemical reaction, cations in the pore solution, such as Na^+, K^+, and Ca^{2+}, moved toward the cathode, while anions, such as OH^-, moved toward the anode. Under natural conditions Ca^{2+} and OH^- ions resulting from dissolution move in the same direction. Thus with this experimental arrangement, the OH^- ions move in the wrong direction. Further, a small current (of several mA) flows during the test, so water electrolysis occurs at the same time at both electrodes, forming a few H^+ and OH^- ions and producing H_2 and O_2 gases. This does not occur under natural conditions. Nevertheless, these differences do not affect the dissolution mechanism, but only influence ion transport efficiency and solubility because of the different pH conditions. Consequently, this method of acceleration with an electric field produces leached samples in a short time without altering the assumed degradation mechanism as given in the reference material[1～5] for the leaching of cement-based materials in water.

3. EXPERIMENT

3.1 Types of test

The study consisted of three different tests: two on mix proportion and one on cement type. These were classified into two groups, as shown in Table 1. In the first group, the sand content was varied to clarify the effect of cement hydrate quantity on the test results. In the other, the water/cement ratio and cement type were varied to clarify the effect of cement hydrate quality on the test results.

Table 1 Characterization of tests

(1) Quantity of cement hydrate	1) Test on different sand contents
(2) Quality of cement hydrate	1) Test on different water/cement ratios 2) Test on various cement types

Table 2 Chemical composition of cements

	Ig.loss	Insol	CaO	SiO_2	Al_2O_3	Fe_2O_3	MgO	SO_3	Na_2O	K_2O
OP	1.82	<0.1	64.0	20.8	4.87	2.90	1.97	2.9	0.30	0.38
MH	0.86	<0.1	64.0	23.3	4.20	4.16	1.11	2.0	0.12	0.24
SO	0.85	<0.1	64.8	22.4	3.70	4.97	0.97	1.9	0.14	0.23
LH	1.46	<0.1	62.5	25.1	3.80	3.72	0.99	2.0	0.14	0.26
B	1.02	<0.1	54.5	25.5	8.91	1.60	4.51	3.1	0.36	0.46

OP : Ordinary Portland cement, MH : Moderate-heat Portland cement,
SO : Sulfate resisting cement, LH : Low-heat Portland cement,
B : Blast-furnace slag cement

Table 3 Composition of clinker (%)

	C_3A	C_3S	C_2S	C_4AF	$CaSO_4$
OP	8	57	16	9	5
SO	4	44	34	13	3
MH	1	56	22	15	3
LH	4	27	52	11	3

Table 4 Mix proportion of mortar

Type of test		W/C	S/C
Test on different sand contents	No.1	0.41	1.62
	No.2		1.00
	No.3		0.57
	No.4		0.25
Test on different water/cement ratios	No.5	0.32	0.67
	No.6	0.41	0.77
	No.7	0.50	0.87
	No.8	0.60	0.97
Test on various cement types (No.9~13)		0.65	2.0

3.2 Mortar specimens

Five cement types were used: ordinary Portland cement (OP), moderate-heat Portland cement (MH), sulfate-resisting cement (SO), low-heat Portland cement (LH), and blast-furnace slag cement (B). The chemical compositions of these cements are given in Table 2, and the clinker mineral contents as calculated by Bouge's equation are given in Table 3. Only OP cement was used in the mix proportion test. The sand was Toyoura Sand (as specified in the former JIS standards; solid volume ratio is 57.2%) in every test. Table 4 shows the mix proportions of the mortar specimens. In the test with different cement types, the water/cement ratio was 0.65 and the sand/cement ratio was 2.0. In the sand content test, the water/cement ratio was 0.41 and four sand/cement ratios were used: 1.62, 1.00, 0.57, and 0.25. These ratios were chosen to achieve four levels of S/Slim (sand volume (S) divided by solid volume ratio (Slim)): 80, 60, 40, and 20%. In the water/cement ratio test, the ratios, 0.32, 0.41, 0.5, and 0.6 were chosen and S/Slim was held constant at 50%. The resulting sand/cement ratios were from 0.67 to 0.97. Certain admixtures were added so as to obtain a flow of about 200 mm as occasion demanded.

The specimens were cylindrical with dimensions 2.5 cm in diameter and 10 cm high. The mortar was cast in cylindrical molds and efficiently compacted using a vibrator. The specimens were cured in water at 20℃ for four weeks.

3.3 Measurements and procedures

a) Cement hydrate structure prior to test
After curing, the characteristics of the cement hydrate structure were measured using a method proposed by Suzuki et. al. [7]. The hydrate constituent was measured by X-ray diffraction, the $Ca(OH)_2$ and $CaCO_3$ contents by TG-DTA, and the Ca/Si molar ratio of C-S-H by chemical analysis. Pore volume and pore distribution within the range 3 nm to 60 μm in diameter were measured by the mercury intrusion method.

b) Leaching acceleration tests
The leaching acceleration tests were carried out by the proposed electrochemical method under the conditions indicated in Table 5. Chemical

Table 5 Test conditions

Potential gradient	10 V/cm
Water	Ion-exchanged water
Temperature	Room temperature (about 25℃)
Test period	Cement types : 3 and 6 months
	Mix proportion : 4 months

reaction rates, such as the dissolution of cement hydrates, are strongly influenced by temperature. To exclude any temperature influence, the tests were carried out in an air-conditioned room at 25℃. Monitoring indicated that the temperature of the solution on the cathode side occasionally increased by about 2℃, but for most of the test period it was maintained at 25℃.

The test periods were 3 and 6 months in the tests of cement type, and 4 months in the mix proportion tests. Test periods were varied so as to obtain suitable degradation thicknesses for the study of changes in concrete performance due to degradation: 2.5 cm is needed for studies of compressive strength in the cement type test and 2.0 cm for gas permeability studies in the mix proportion test.

The solutions on both anode and cathode sides were replaced once a week, and the Ca^{2+} concentration in the cathode solution was measured by atomic absorption analysis. After the acceleration test, the specimens were removed from the apparatus and the degradation thickness measured. The degraded region was easily distinguished visually, because of the density change resulting from cement hydrate dissolution.

c) Change in hydrate structure after acceleration test
Each specimen was divided into two pieces by cutting at the degradation boundary using a diamond cutter. The mineral composition and pore volume were measured using the method described in a) above for each piece.

d) Mortar performances after acceleration test
Compressive strength and gas permeability were measured to estimate the change in concrete performance resulting from degradation. The specimens used to measure compressive strength were about 2.5 cm long and the gas permeability specimens were about 2 cm long.

Gas permeability was measured using a method proposed by Nagataki and Ujike [8] after one week of vacuum drying, and the permeability coefficients were calculated from the following equation:

$$K = 2l \times Q \times A \times P_2 \gamma / (P_1^2 - P_2^2) \qquad (3)$$

where, K: gas permeability coefficient (cm/s)
l: length of specimen (cm)
Q: flowing air volume (cm^3/s)
A: area of specimen (cm^2)
γ : unit weight of air (1.205×10^{-6} kg/cm^3)
P_1: loading pressure (Pa)
P_2: atmospheric pressure (Pa)

Table 6 $Ca(OH)_2$ and $CaCO_3$ content and Ca/Si molar ratio of C-S-H

		$Ca(OH)_2$ [%]	$CaCO_3$ [%]	Ca/Si molar ratio of C-S-H	Remarks
Sand content	No.1	19.4	7.7	2.0	S/C:1.62
	No.2	18.7	7.7	2.1	S/C:1.0
	No.3	19.5	7.8	1.9	S/C:0.57
	No.4	19.9	8.0	2.0	S/C:0.25
Water/cement ratio	No.5	17.0	9.1	1.9	W/C:0.32
	No.6	18.7	8.2	2.0	W/C:0.41
	No.7	21.3	8.4	1.9	W/C:0.5
	No.8	21.4	9.8	1.9	W/C:0.6
Cement type	No.9	21.2	7.7	2.0	OP
	No.10	19.6	6.8	2.0	MH
	No.11	21.9	7.2	1.9	SO
	No.12	12.3	6.7	2.1	LH
	No.13	7.8	5.0	2.0	B

Table 7 Pore volume at beginning of test

		PV [cc/cc]	PV/Vp [cc/cc]	Remarks
Sand content	No.1	0.164	0.303	S/C:1.62
	No.2	0.169	0.257	S/C:1.0
	No.3	0.184	0.238	S/C:0.57
	No.4	0.226	0.254	S/C:0.25
Water/cement ratio	No.5	0.145	0.203	W/C:0.32
	No.6	0.171	0.240	W/C:0.41
	No.7	0.240	0.336	W/C:0.5
	No.8	0.253	0.354	W/C:0.6
Cement type	No.9	0.206	0.368	OP
	No.10	0.223	0.397	MH
	No.11	0.208	0.371	SO
	No.12	0.204	0.362	LH
	No.13	0.193	0.342	B

PV : Pore volume per unit specimen volume (same in following table)
PV/Vp : Pore volume per cement paste volume(same in following table)

4. CEMENT HYDRATE STRUCTURE PRIOR TO TEST

4.1 Mineral composition of hydrated product

Every specimen contained $Ca(OH)_2$, C-S-H, and monosulfate. This was verified by X-ray diffraction. The $Ca(OH)_2$ and $CaCO_3$ content and the Ca/Si molar ratio of C-S-H for each specimen are shown in Table 6. In the sand content test, the $Ca(OH)_2$ content was 18.7% to 19.9% and the $CaCO_3$ content was 7.7% to 8.0%. These values are similar and independent of the sand content. In the water/cement ratio test, the $Ca(OH)_2$ content was 17.0% to 21.4%. It was similar for water/cement ratios of 50 and 60%, but seemed to decrease slightly with the water/cement ratio. The $CaCO_3$ content was 8.2% to 9.8%, and was independent of the water/cement ratio.

In the cement type test, the $Ca(OH)_2$ content varied with cement type. It was similar (21.2% and 21.9%, respectively) in the case of ordinary

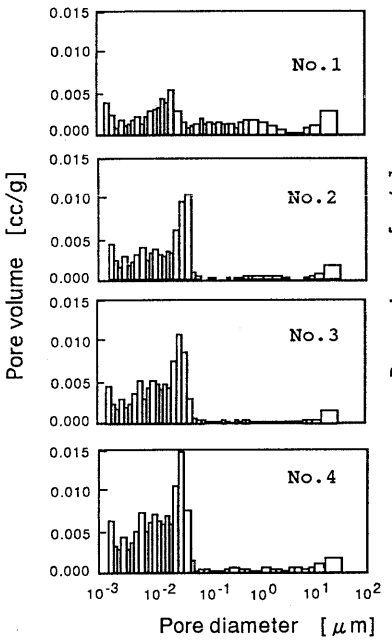

Fig.2 Pore distribution (S/C)

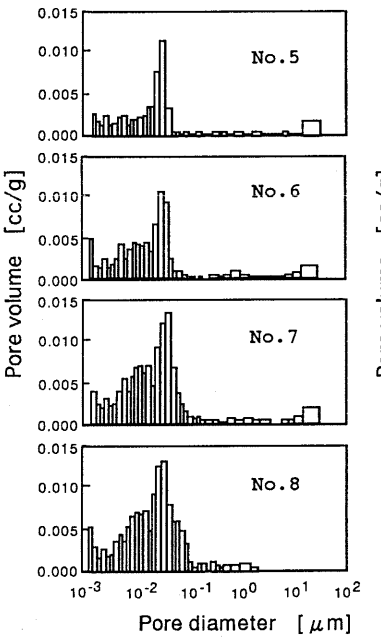

Fig.3 Pore distribution (W/C)

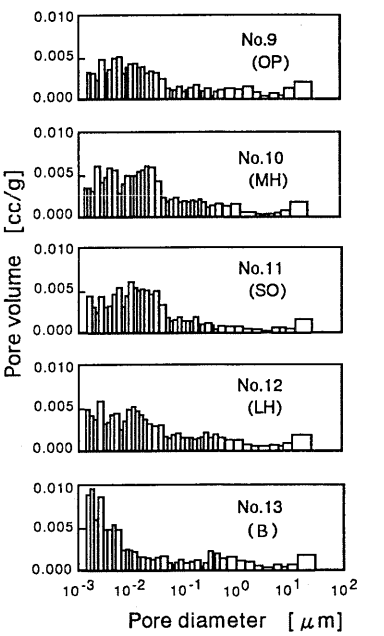

Fig.4 Pore distribution (Cement)

Portland cement and sulfate-resisting cement, 19.6% in moderate-heat Portland cement, and 7.8% in blast-furnace slag cement. This difference can be attributed to the different clinker mineral constituents. The Ca/Si molar ratio of C-S-H was 1.9 to 2.1, and was similar for each cement type and mix proportion.

4.2 Pore structure

Table 7 shows the pore volume of each specimen. Cement hydrate contents vary with the mix proportion. The PV/Vp value, pore volume divided by volume of cement paste, is also shown in Table 7 to allow a comparison of the pore structures. In the sand content test, PV/Vp was similar for sand/cement ratios under 1, but it was 20% higher with a sand/cement ratio of 1.62. It is deduced from the pore distribution, which is described later, that the difference in PV/Vp is due to the formation of a transit zone. In the water/cement ratio test, PV/Vp increased with water/cement ratio within the range 0.2 to 0.35, indicating that cement hydrate structure became coarser with increasing water/cement ratio. In the cement type test, PV/Vp varied little, ranging from 0.34 to 0.4.

The pore distributions are shown in Figs. 2 to 4. In the sand content test, the distribution was similar for sand/cement ratios under 1, with most pores under 50 nm in diameter. However, for the sand/cement ratio of 1.62 there were also pores of 50 nm to 2 μm in diameter. It has been reported that pores in this size range result from a transition zone formed around sand particles [9]. In the water/cement ratio test, most pore diameters were below 50 nm, because the sand/cement ratio was under 1. Generally, there were many pores of 20 to 50 nm in diameter for sand/cement ratios under 1. In the cement type test, distributions were similar for the Portland cements, but the volume of pores under 5 nm in diameter were much higher in blast-furnace slag cement than in Portland

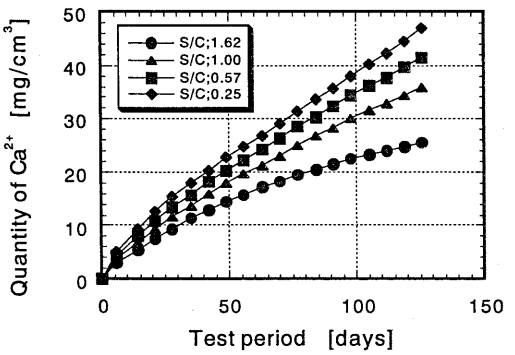

Fig. 5 Cumulative quantity of dissolved Ca^{2+} (1)

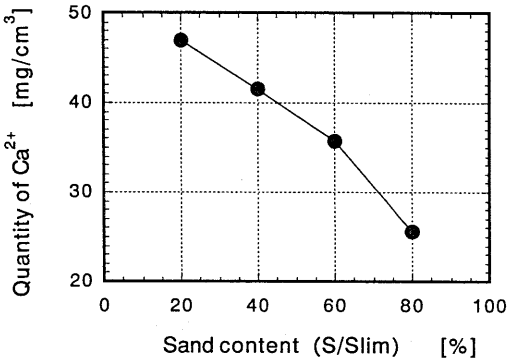

Fig. 6 Relationship between sand content and cumulative quantity of dissolved Ca^{2+}

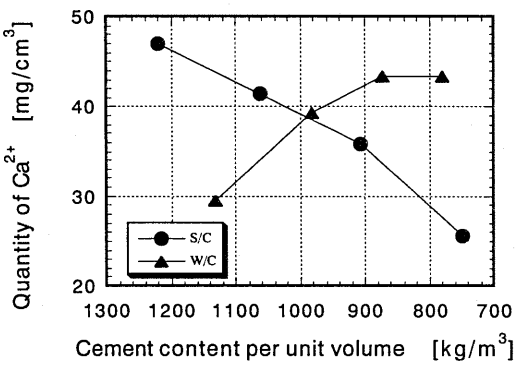

Fig. 7 Relationship between cement content and quantity of dissolved Ca^{2+}

cement. These results correspond with those already reported [10], and it can be said that they reflect the characteristics of the various cement types.

As described above, the characteristics of cement hydrate structure are clearly revealed in the pore volume and the pore distribution, reflecting differences in mix proportion and cement type.

5. QUANTITY OF DISSOLVED Ca^{2+} AND DEGRADED MORTAR THICKNESS

5.1 Quantity of dissolved Ca^{2+}

Fig. 5 shows the cumulative quantity of dissolved Ca^{2+} in the sand content test (per unit mortar volume). It differs for each sand/cement ratio. Thus, the results reflect the differences in cement content per unit mortar volume. This phenomenon is discussed later.

Fig. 6 shows the relationship between the quantity of dissolved Ca^{2+} and sand content (S/Slim). The quantity of Ca^{2+} decreased almost in proportion to sand content. Thus, the decrease rate at 80% of S/Slim is larger than that for the other sand content. This result suggests that the volume of the transit zone may influence the quantity of dissolved Ca^{2+}. Verifying this is a task for the future.

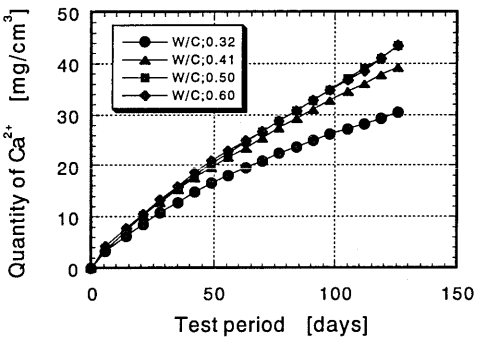

Fig. 8 Cumulative quantity of dissolved Ca^{2+} (2)

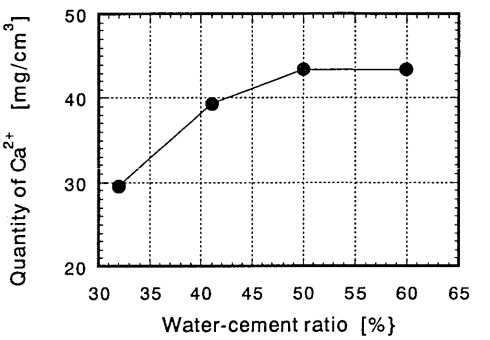

Fig. 9 Relationship between water/cement ratio and quantity of dissolved Ca^{2+}

The greater the sand content, the smaller the cement content per unit volume. The relationship between cement content per unit volume and the quantity of dissolved Ca^{2+} is shown in Fig. 7. Low cement contents are at the right end of the horizontal axis allow comparison with Fig. 6. The quantity of Ca^{2+} decreases almost in proportion to the decrease in cement content, and is very similar to the relationship between the quantity of Ca^{2+} and sand content described above. Therefore, the almost proportional decrease in Ca^{2+} quantity with sand content is due to the decrease in cement content, i.e., the decrease in cement hydrate volume.

Fig. 8 shows the cumulative quantity of Ca^{2+} dissolved in water in the water/cement ratio test and Fig. 9 shows the relationship between water/cement ratio and the quantity of Ca^{2+} dissolved in water. The quantity of dissolved Ca^{2+} increases with the water/cement ratio, but the increase is very small at ratios over 50%. The smaller the water/cement ratio, the greater the cement content per unit volume. The results obtained in this test are also plotted in Fig. 7. The quantity of Ca^{2+} decreases with cement content in this test. This is the opposite of the test results for sand content, and demonstrates that the quantity of dissolved Ca^{2+} is affected not only by the quantity of cement hydrates but also by the quality of the hydrates. That is, the tighter the cement hydrates, the smaller the quantity of Ca^{2+}.

In neither test quantity of dissolved Ca^{2+} is explained by the cement content per unit volume or water/cement ratio alone. This shows that a new indicator incorporating both the quantity and quality of cement hydrates is needed. We assume that Ca^{2+} ions move through continuous pores in the cement hydrate structure. The pore volume per unit mortar volume is equivalent to the pore area per unit area. This value could thus be taken as the new index. Table 8 shows the pore volume of the undegraded part of specimens after testing, and Fig. 10 shows the relationship between the quantity of dissolved Ca^{2+} and a value equivalent to pore area per unit mortar area. It is observed that the quantity of Ca^{2+} increases with pore area. This index may thus be useful in explaining the quantity of Ca^{2+} dissolved in water. However, it also seems that the relationship is different from that of water/cement ratio, and the plot for a sand/cement ratio of 1.62 when a transit zone forms is inconsistent with the relationship. This indicates the need for another index that takes into account the pore distribution. This new index is introduced here. It is equivalent to pore number, or the pore area divided by the

Table 8 Pore volume of undegraded part after test

		PV [cc/cc]	Average pore radius [$10^{-3}\mu$m]	N* [10^{11}/g]	Remarks
Sand content	No.1	0.142	6.8	0.98	S/C:1.62
	No.2	0.139	5.8	1.32	S/C:1.0
	No.3	0.166	5.8	1.57	S/C:0.57
	No.4	0.185	5.8	2.10	S/C:0.25
Water/cement ratio	No.5	0.123	5.1	1.51	W/C:0.32
	No.6	0.150	6.1	1.28	W/C:0.41
	No.7	0.210	6.3	1.69	W/C:0.5
	No.8	0.244	6.9	1.63	W/C:0.6
Cement type	No.9	0.196	6.5	1.47	OP
	No.10	0.210	7.0	1.36	MH
	No.11	0.204	7.3	1.22	SO
	No.12	0.202	6.5	1.52	LH
	No.13	0.181	4.2	3.21	B

* ; A new index for comparing number of pores per unit area (=PV/circular area with average pore radius)

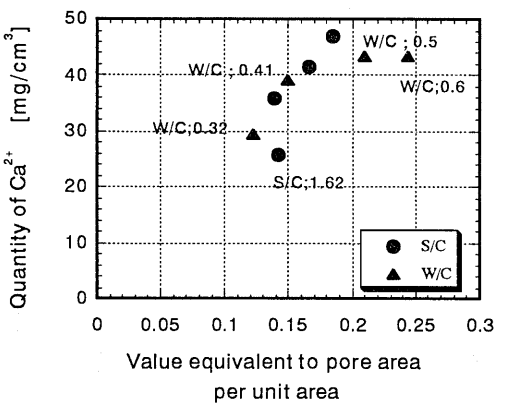

Fig. 10 Relationship between value equivalent to pore area per unit area and quantity of dissolved Ca^{2+}

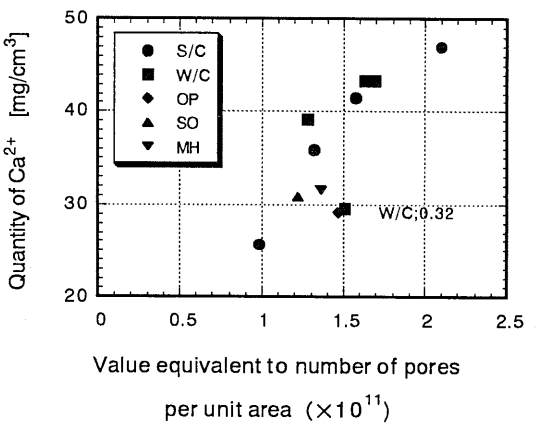

Fig. 11 Relationship between value equivalent to number of pores per unit area and quantity of dissolved Ca^{2+}

circular pore area with the average radius obtained from the pore distribution. Its value is given in Table 8, and the relationship between it and the quantity of dissolved Ca^{2+} is shown in Fig. 11. There is good correspondence except for the datum for a water/cement ratio of 32%, and the quantity of Ca^{2+} increases with pore number. Differences in the quantity of Ca^{2+} can be explained clearly by the new index. The new index also takes into account the varying quantity and quality of cement hydrates, which corresponds to differences in the mix proportion. Differences in mix proportion are thus revealed.

Fig. 12 shows the cumulative quantity of dissolved Ca^{2+} for the cement type test. The Ca content per unit volume differs somewhat depending on cement type, so the data are corrected using the chemical composition shown in Table 2 to allow comparison with ordinary Portland cement. The data for the Portland cements are similar. After 6 months, the amounts

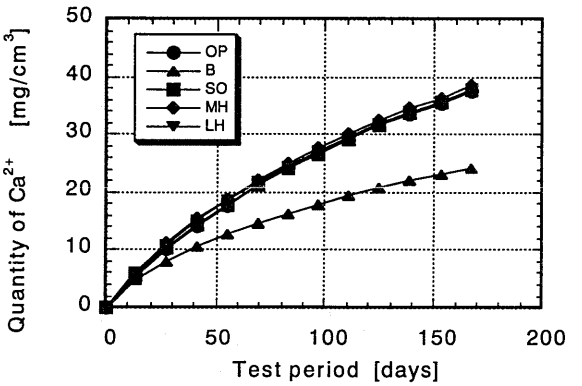

Fig.12 Cumulative quantity of dissolved Ca^{2+} (3)

Table 9 Degradation thickness

		Degradation thickness [mm]	Quantity of Ca^{2+} dissolved in water [mg]	Remarks
Sand content	No.1	14.4	1,258	S/C:1.62
	No.2	15.2	1,757	S/C:1.0
	No.3	15.5	2,034	S/C:0.57
	No.4	15.8	2,303	S/C:0.25
Water/cement ratio	No.5	11.2	1,449	W/C:0.32
	No.6	15.5	1,925	W/C:0.41
	No.7	21.3	2,130	W/C:0.5
	No.8	22.1	2,128	W/C:0.6
Cement type	No.9	26.3(17.3)	1,755(1,165)	OP
	No.10	29.8(21.3)	1,887(1,282)	MH
	No.11	27.3(16.0)	1,853(1,156)	SO
	No.12	31.0(19.3)	1,776(1,197)	LH
	No.13	26.0(19.0)	1,188(843)	B

( ) ; test results after 3months

of Ca^{2+} in sulfate-resisting and moderate-heat Portland cement are about 8% higher than those for ordinary Portland cement and low-heat Portland cement. However, the value is about 30% less for blast-furnace slag cement. Because differences in the amount of Ca^{2+} in the water depend not only on the cement hydrate composition but also on the tightness of the cement hydrate structure, the quantity of dissolved Ca^{2+} after 4 months was estimated and the results are plotted in Fig. 11. The data for Portland cement with the same $Ca(OH)_2$ content can be explained using the same new index, but the data for blast-furnace slag cannot be explained. This result suggests that there is a necessity to consider the mineral constitution of the cement hydrates. This is a task for the future.

5.2 Degradation thickness of mortar

Table 9 shows the results of tests on the degradation thickness of the mortar and the quantity of Ca^{2+} dissolved. The thickness of the degraded section decreased gradually with increasing sand content in the sand content test. However, in the water/cement ratio test, it first increased steeply with water/cement ratio, but leveled off above 50%. In the

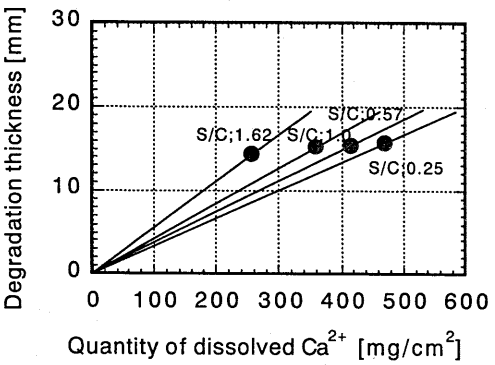

Fig. 13 Relationship between quantity of dissolved Ca^{2+} per unit area and degradation thickness

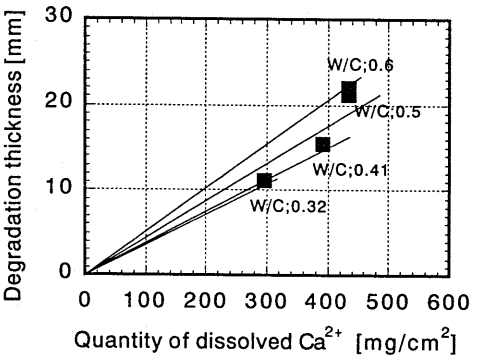

Fig. 14 Relationship between quantity of dissolved Ca^{2+} per unit area and degradation thickness

Table 10 Constants for each line

	W/C	S/C	Vc*1	k1*2	k1×k2*3
No.1	0.41	1.62	0.236	1.337	0.0562
No.2	0.41	1.00	0.286	1.103	0.0463
No.3	0.41	0.57	0.335	0.942	0.0396
No.4	0.41	0.25	0.385	0.819	0.0344
No.5	0.32	0.67	0.357	0.884	0.0371
No.6	0.41	0.77	0.310	1.018	0.0428
No.7	0.50	0.87	0.275	1.147	0.0482
No.8	0.60	0.97	0.246	1.282	0.0538

*1; Cement volume ratios in the specimen
*2; Constants determined by mix proportions: $1/(Vc \times \rho c)$
*3; Calculation assuming k2=0.042[3)]

cement type test, the thickness depended on the cement type. With blast-furnace slag cement and sulfate-resisting cement, the thickness of the degradation was similar to that for ordinary Portland cement, while for moderate-heat and low-heat Portland cement it was 15% to 20% higher. As reported in another paper [3], the relationship between the quantity of dissolved Ca^{2+} per unit area (TCa/S) and the degradation thickness of the mortar (DL) can be expressed by the following linear equation:

$$DL = k1 \times k2 \times TCa/S \qquad (4)$$

where, k1: a constant determined by mix proportions
k2: a constant determined by cement hydrate constituents

Figs. 13 and 14 show the relationship between the degradation thickness and the quantity of dissolved Ca^{2+} in the sand content test and the water/cement ratio test, respectively. Lines given by equation (4) are shown in each figure. Table 10 shows the constants for each line. The data obtained in each test are also plotted and fall on each line. This demonstrates that the relationship obtained by the test is equivalent to that expressed by equation (4).

Fig. 15 shows the same relationship for the cement type test. The data obtained after 3 months are also plotted to clarify the effect. Good correlation is shown for each cement type.

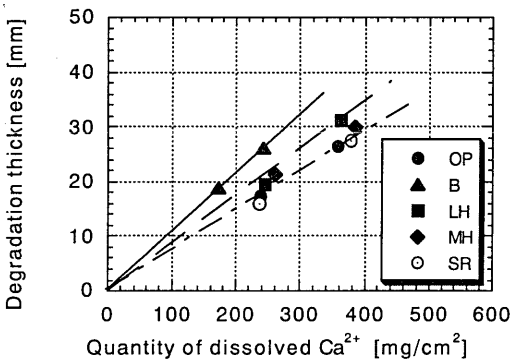

Fig. 15 Relationship between quantity of dissolved Ca^{2+} per unit area and degradation thickness

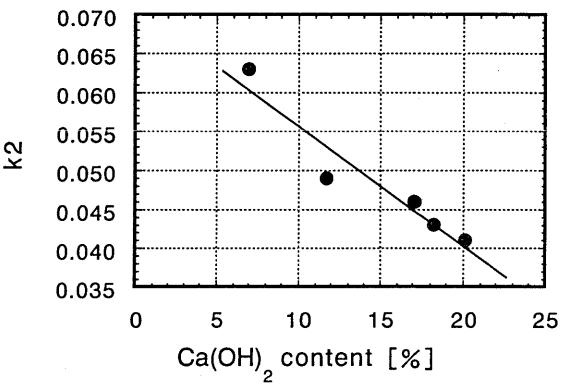

Fig. 16 Relationship between $Ca(OH)_2$ content and k2

Table 11 $Ca(OH)_2$ contents, slope coefficients, k1, and k2

	$Ca(OH)_2$ [%]	k1×k2*1	k1	k2
No.2	18.7	0.0425	1.103	0.0385
No.3	19.5	0.0374	0.942	0.0397
No.4	19.9	0.0337	0.819	0.0411
No.5	17.0	0.0380	0.884	0.0429
No.8	21.4	0.0509	1.282	0.0397
No.12	12.3	0.0867	1.72	0.0504
No.13	7.8	0.1085	1.72	0.0631

*1; The slope coefficients of each line shown in Figs.13 to 14

These results suggest that differences in degradation thickness result from differences in mix proportion, cement hydrate composition, and quantity of dissolved Ca^{2+}. Differences in mix proportion and cement type are reflected in the degradation thicknesses obtained in the tests.

In equation (4), k2 is a constant determined from the constituents of the cement hydrates. Here, we discuss the relationship between k2 and the $Ca(OH)_2$ content. The focus is placed on $Ca(OH)_2$ content because it is considered to be closely related to the degradation thickness. This is because the degradation occurs in the region where all $Ca(OH)_2$ in the cement hydrate has already dissolved. The different $Ca(OH)_2$ content specimens were selected from the data shown in Table 6. K2 is calculated from k1 and the slope coefficients of each line shown in Figs. 13 to 14. These values and the $Ca(OH)_2$ contents are shown in Table 11, and the relationship between k2 and the $Ca(OH)_2$ content is shown in Fig. 16. They show good correlation, and k2 decreases with $Ca(OH)_2$ content. Therefore, it can be said that k2 is determined by $Ca(OH)_2$ content.

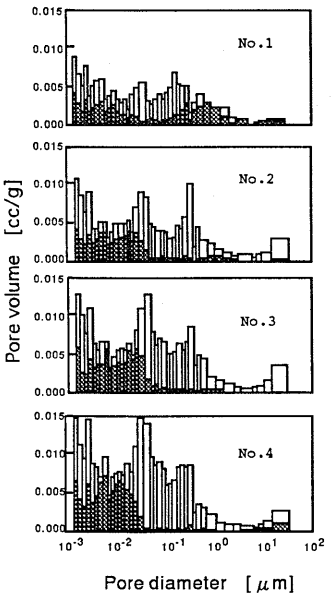

Fig.17 Pore distribution (S/C)
(Hatched : undegraded;
unhatched: degraded)

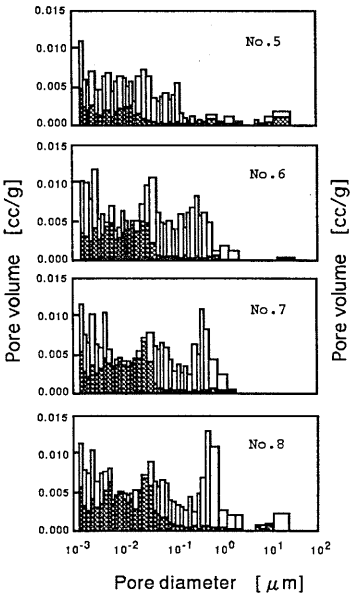

Fig.18 Pore distribution (W/C)
(Hatched : undegraded;
unhatched: degraded)

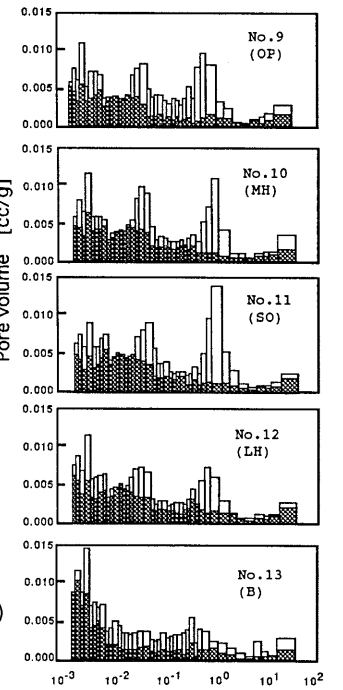

Fig.19 Pore distribution (cement)
(Hatched : undegraded;
unhatched: degraded)

6. DEGRADATION OF SPECIMEN

6.1 Visual inspection

The degraded regions could be clearly distinguished visually, because they were coarser than the undegraded regions. There were no visible differences in degraded appearance for different mix proportions and cement types.

6.2 Changes in cement hydrate constituents

Based on the results obtained by X-ray diffraction and TG-DTA, the main minerals were confirmed to be $Ca(OH)_2$, C-S-H, and monosulfate in the undegraded region, but only C-S-H in the degraded region. These results correspond with those reported previously [1,2].

6.3 Pore volume and pore distribution

The pore volumes and distributions obtained from the acceleration test are shown in Table 12 and Figs. 17 to 19, respectively. The pore volumes in the undegraded regions were 5% to 15% less than those obtained at the beginning of the acceleration test. This shows that the cement hydrate structure became tighter during the 4- to 6-month test period.

From the viewpoint of the change in pore distribution, it can be pointed out that the volume of pores in the range of 20 to 50 nm in diameter, which is the characteristic distribution for sand/cement ratios under 1,

Table 13 Gas permeability coefficient

	Degraded		Undegraded		Remarks
	K (10^{-9}) [cm/sec]	K/Vp(10^{-9}) [cm/sec]	K (10^{-10}) [cm/sec]	K/Vp(10^{-10}) [cm/sec]	
No.1	3.65	6.75	17.1	31.6	S/C:1.62
No.2	3.63	5.53	3.19	4.86	S/C:1.0
No.3	3.37	4.37	3.43	4.45	S/C:0.57
No.4	3.92	4.43	4.88	5.51	S/C:0.25
No.5	1.44	2.02	6.07	8.50	W/C:0.32
No.6	3.22	4.51	4.40	6.16	W/C:0.41
No.7	5.75	8.05	9.72	13.6	W/C:0.5
No.8	8.62	12.1	13.0	18.2	W/C:0.6

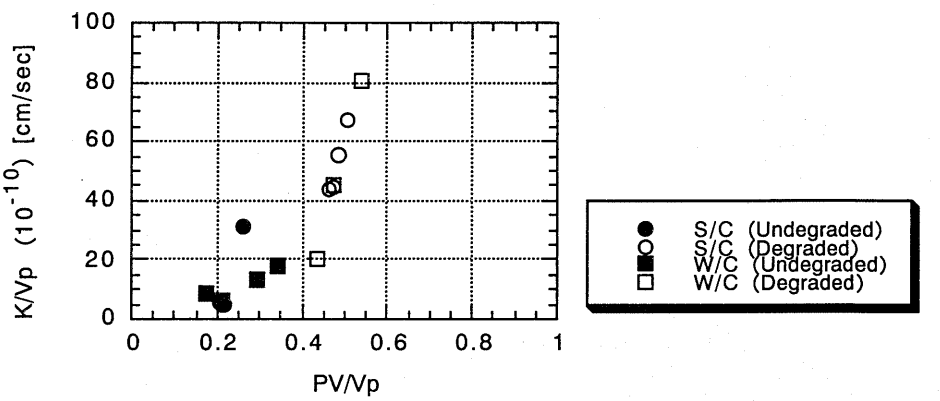

Fig.20 Relationship between PV/Vp and K/Vp

decreased, but there was no large change in pore distribution for sand/cement ratios over 1. Comparing undegraded with degraded regions, the pore volume increased by about two times in the sand content test and water/cement ratio test, and by 60% in the cement type test. This shows that the cement hydrate structure became coarser with leaching. Pore volumes increased markedly, not only for pores under 5 nm in diameter and in the range 500 nm to 1 μ m in diameter, as reported before [2], but also in the range 50 to 500 nm in diameter in most specimens. However, the pore volume increased homogeneously over all diameter ranges in the case of blast-furnace slag cement. These results suggest differences in cement hydrate structure. This is a very interesting phenomenon, and is a subject for future study.

6.4 Relationship between pore structure and gas permeability

It was clarified that the volume of pores over 50 nm in diameter increased with degradation. It has also been shown that ion permeability correlates closely with the volume of pores over 50 nm in diameter [11]. Thus, the ability to prevent nuclide movement, one of the most important features of a repository, would fall in degraded regions. Table 13 shows the gas permeability of the undegraded and degraded specimens. We adopt a new value, K/Vp (gas permeability divided by cement paste volume), as a new index of permeability to interpret changes in cement hydrate structure due to dissolution from the viewpoint of gas permeability.

Table 14 Compressive strength N/mm²

	Degraded	Undegraded	Standard curing	Remarks
No.9	9.21	45.3	43.9	OP
No.10	11.8	44.5	47.4	MH
No.11	10.5	40.4	40.2	SO
No.12	14.9	47.6	44.7	LH
NO.13	20.1	48.3	48.0	B

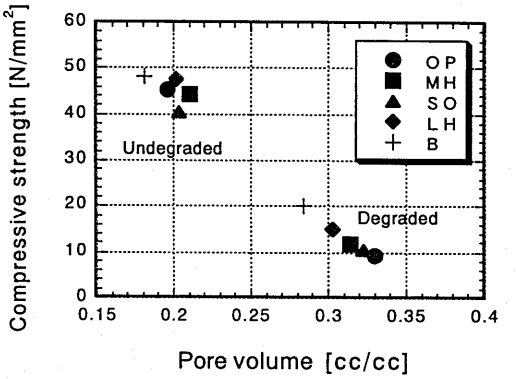

Fig. 21 Relationship between pore volume and compressive strength

Fig. 20 shows the relationship between K/Vp and pore volume per cement paste volume. They show good correlation. PV/Vp was within the range 0.2 to 0.35, and K/Vp increased slightly with PV/Vp, except in the case of the datum for a sand/cement ratio of 1.62 in the undegraded specimen. The value in this case was 6 times larger than the others, a result that could be due to the formation of a transit zone. PV/Vp was over 0.4, and K/Vp increased almost proportionally with PV/Vp and independently of mix proportion in the degraded specimen. This result indicates that the pores formed by dissolution are continuous.

These results support the hypothesis [11] that permeability is closely correlated to the volume of pores 50 to 500 nm in diameter.

7. RELATIONSHIP BETWEEN COMPRESSIVE STRENGTH AND DEGRADATION

Table 14 shows compressive strengths after a 6-month acceleration test using various cements and after the same period of standard curing. The compressive strength of undegraded specimens was the same as that of standard-cured specimens. However, the compressive strength of degraded specimens was 20% to 40% that of the standard-cured specimens. This clarifies that compressive strength decreases greatly with dissolution of the cement hydrates. Fig. 21 shows the relationship between compressive strength and pore volume. It is clearly seen that the compressive strength decreases as the pore volume increases. Thus, the loss of strength is caused mainly by a change in the cement hydrate structure to a porous structure due to dissolution of hydrates.

8. CONCLUSIONS

An electrochemical acceleration test method has been developed. A potential gradient is applied across specimens to accelerate the dissolution of cement hydrates from concrete in contact with water. Experimental studies were carried out to clarify the effect of differences in cement types and mix proportions, and these effects were reflected in the way results of the test are analyzed. Sand content tests were carried out to determine differences in the quantity of cement hydrates. Water/cement ratio tests and cement types tests were carried out to determine differences resulting from cement hydrate quality. Results were analyzed from the viewpoint of the quantity and quality of the cement hydrates.

The results were as follows.

(1) The characteristics of the cement hydrate structure reflect differences in mix proportion and cement type. Differences were observed in cement hydrate constituents and pore distribution at the beginning of the acceleration tests.

(2) The amount of Ca^{2+} entering the water varied with the mix proportion and cement type. It decreased with sand content, but increased with water/cement ratio. It was similar for the Portland cements, but was 30% less for blast-furnace slag cement.

The above results were attributed to differences in the quantity and quality of the cement hydrates. A new index, equivalent to the pore number per unit area, was introduced based on the assumption that Ca^{2+} ions moved through continuous pores in the cement hydrate. That is, it is the pore volume per unit mortar volume divided by a circular area based on the average pore radius obtained from the pore distribution, since the pore volume per unit mortar volume is equivalent to the pore area per unit area. The new index, which takes into account the quantity and quality of cement hydrates, explains the difference in the amount of dissolved Ca^{2+} . It was thus deduced that differences in mix proportion and cement type are in fact reflected in the amount of Ca^{2+} entering the water.

(3) The degradation thickness decreased slightly with increasing sand content, but increased greatly with water/cement ratio. It also varied with cement type.

As previously reported, the relationship between degradation thickness (DL) and the amount of dissolved Ca^{2+} per unit area (TCa/S) can be expressed by the linear equation given below. This relation was verified by these test results, and differences in degradation thickness were attributed to differences in mix proportion, cement hydrate constituents, and the amount of dissolved Ca^{2+}. The equation expresses these differences.

$$DL = k1 \times k2 \times TCa/S$$

where k1 is a coefficient determined from the mix proportion and k2 is a coefficient determined from the cement hydrate constituents.

(4) The pore volume in the degraded specimens increased by 1.6 to 2 times compared with that in the undegraded specimen. The volumes of pores under 5 nm in diameter and from 50 nm to 1É m in diameter increased greatly, except with blast-furnace slag cement and with a low water/cement ratio of 0.31.

(5) The gas permeability of the mortar increased almost in proportion to pore volume due to degradation. It is thus deduced that the pores are continuous and that the permeability of the degraded region increases according to the change in characteristic pore distribution described in (4) above.

(6) The compressive strength of the degraded mortar specimens fell to 20~40% that of the undegraded mortar. There is good correlation between pore volume and compressive strength. It is thus deduced that the loss of strength was due to an increase in the pore volume.

Acknowledgments

The authors greatly appreciate the assistance of Prof. Maekawa (Tokyo Univ.) who advised them on the mix proportion test. The tests on various types of cement were carried out with the cooperation of the Radioactive Waste Management Center (RWMC) and the authors thank the members of the concrete committee of the RWMC.

References

[1] Saito, H., Nanake, S., and Fujiwara, A. "Effect of Electrical potential Gradients on Dissolution and Deterioration of Cement Hydrate by Electrical Acceleration Test Method," Concrete Research and Technology, Vol. 4, No. 2, July 1993 (in Japanese)
[2] Saito, H., Nanake, S., and Fujiwara, A. "Application of Electrical Acceleration Test Method to Deterioration of Cement Hydrate by Leaching Ca^{2+}," Annual Report of Concrete Research and Technology, Vol. 16, No. 1, 1994 (in Japanese)
[3] Saito, H., Nanake, S., and Fujiwara, A. "Relationship between Deteriorated Region of Cement Hydrate and Accumulated Leached Ca^{2+} in Electrical Acceleration Test Method," Annual Report of Concrete Research and Technology, Vol. 17, No. 1, 1995 (in Japanese)
[4] GÈrard, B., "Contribution des Couplages MÈchanique-Chimie-Transfert Dans la Tenue a Long Terme des Ouvrages de Stockage de DÈchets Radioactifs," thÈse de doctorat ENS Cachan/Univ. Laval-QuÈbec, 1996
[5] A. Gerdes and F.H. Wittmann, "Electrochemical Degradation of Cementitious Materials," Proc. 9th International Congress on the Chemistry of Cement, New Dehli, 1992
[6] P. W. Brown and J. R. Clifton, "Mechanisms of Deterioration in Cement-Based Materials and in Lime Mortar," Durability of Building Materials, 1998
[7] Suzuki, K., Nisikawa, N., Yamade, Y, and Taniguti, I., "Analysis of Hydrated Phases for Evaluating the Durability of Concrete," Concrete Research and Technology, Vol. 1, No. 2, July 1990 (in Japanese)
[8] Nagataki, S. and Ujike, I., "Gas Permeability of Concrete," Cement and Concrete, 1985 (in Japanese)
[9] Uchikawa, H., "Similarity and Difference of Mortar and/or Concrete from the Viewpoint of Constituents and Structure," Cement and Concrete, 1989 (in Japanese)
[10] Uchikawa, H., "Effect of Admixtures on Hydration of Blended Cement and its pore structure," Cement and Concrete, 1987 (in Japanese)
[11] Habara, T., "Structure of Concrete and its Performance," Cement and Concrete, 1992 (in Japanese)